# Supplementary Informations

## Reassembling nanometric magnetic subunits into secondary nanostructures with controlled interparticle spacing

Koushik Saikia[1], Debasis Sen[2], Subhasish Mazumder[2] and Pritam Deb[1]*

[1] Advanced Functional Material Laboratory (AFML), Tezpur University (Central University), Tezpur, India.

[2] Solid State Physics Division, Bhabha Atomic Research Centre, Mumbai 400085, India.

**ESI 1:** The figure S1 shows the FTIR of $IO_{NPs}$@OA. The binding of oleic acid molecules to the nanoparticle surface through carboxylate group is confirmed from the asymmetric $\nu_{as}(COO^{-})$ and $\nu_{s}(COO^{-})$ symmetric stretching vibrations at 1619 $cm^{-1}$ and 1525 $cm^{-1}$ respectively.[1] The chelating bidentate binding configuration is ensured from the obtained splitting difference $\Delta$ (1619-1525 $cm^{-1}$ = 99 $cm^{-1}$ < 110 $cm^{-1}$) of these two stretching modes. The band at 1414 $cm^{-1}$ is attributed to the bending vibration of $CH_3$.[2] The band observed at 573 $cm^{-1}$ corresponds to vibration of the Fe–O functional group.[3] Two bands at 2915 $cm^{-1}$ and 2854 $cm^{-1}$ are attributed to the asymmetric $CH_2$ stretching and the symmetric $CH_2$ stretching respectively.[1]

**Figure S1.**

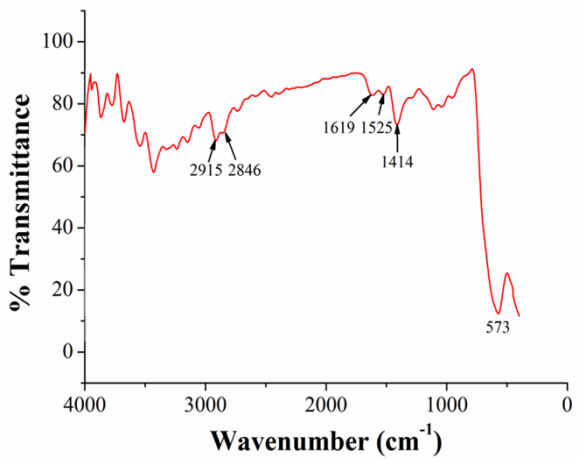

**ESI 2: Zeta potential Measurement**: For zeta potential measurement both $IO_{agg}$@CTAB and $IO_{NPCs}$@PAA samples were diluted to same concentration. Zeta cells were equilibrated at 25 ºC for two minutes before recording three measurements each of ten runs. Data was collected with automatic attenuation selected and analysed using the Smoluchowski model. Zeta potential of PAA was measured in the pH range 2 to 13.

Figure S2 (a), (b) and (c) show the zeta potential of $IO_{agg}$@CTAB, PAA and $IO_{NPCs}$@PAA respectively.

**Figure S2 (a):**

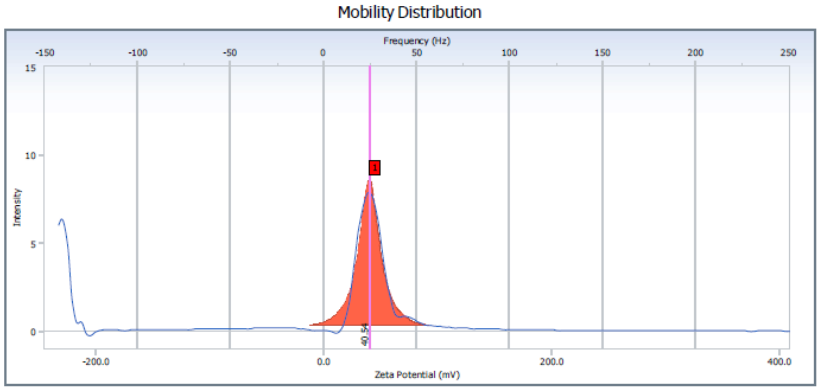


Measurement Results

| | | | | | |
|---|---|---|---|---|---|
| Zeta Potential | : 40.54 | (mV) | Doppler shift | : 24.84 | (Hz) |
| Mobility | : 3.161e-004 | (cm²/Vs) | Base Frequency | : 122.3 | (Hz) |
| Conductivity | : 0.3809 | (mS/cm) | Conversion Equation | : Smoluchowski | |
| Zeta Potential of Cell | | | Diluent Properties | | |
| Upper Surface | : 87.99 | (mV) | Diluent Name | : WATER | |
| Lower Surface | : -0.05 | (mV) | Temperature | : 25.0 | (°C) |
| Cell Condition | | | Refractive Index | : 1.3328 | |
| Cell Type | : Flow Cell | | Viscosity | : 0.8878 | (cP) |
| Avg. Electric Field | : 16.38 | (V/cm) | Dielectric Constant | : 78.3 | |
| Avg. Current | : 0.31 | (mA) | | | |

**Figure S2 (b):**

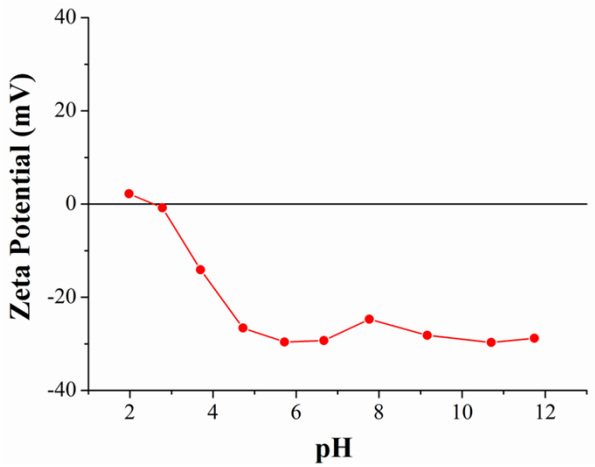

**Figure S 2(c):**

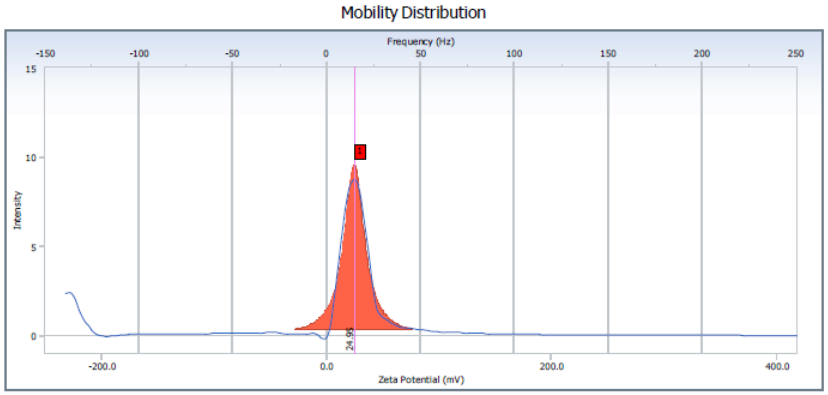


Measurement Results

| | | | | | |
|---|---|---|---|---|---|
| Zeta Potential | : 24.95 | (mV) | Doppler shift | : 14.95 | (Hz) |
| Mobility | : 1.946e-004 | (cm²/Vs) | Base Frequency | : 124.1 | (Hz) |
| Conductivity | : 2.6344 | (mS/cm) | Conversion Equation | : Smoluchowski | |

| | | | | | |
|---|---|---|---|---|---|
| Zeta Potential of Cell | | | Diluent Properties | | |
| Upper Surface | : 63.32 | (mV) | Diluent Name | : WATER | |
| Lower Surface | : 5.02 | (mV) | Temperature | : 25.0 | (°C) |
| Cell Condition | | | Refractive Index | : 1.3328 | |
| Cell Type | : Flow Cell | | Viscosity | : 0.8878 | (cP) |
| Avg. Electric Field | : 16.02 | (V/cm) | Dielectric Constant | : 78.3 | |
| Avg. Current | : 2.11 | (mA) | | | |

## ESI 3: Length scales estimated from SANS

| Systems | Length scales (mu) in nm | Polydispersity(σ) | $f_p$ |
|---|---|---|---|
| $IO_{NPs}$@OA | 58.30 | 0.179 | |
| | 365.04 | 0.274 | |
| | 8.19 | 0.274 | |
| $IO_{agg}$@CTAB | 48.00 | 0.220 | 0.444 |
| | 384.61 | 0.347 | 0.303 |
| | 8.30 | 0.390 | |
| $IO_{NPCs}$@PAA | 55.32 | 0.308 | 0.353 |
| | 410.18 | 0.258 | |

**ESI 4**: Figure S4 shows the XRD pattern of $IO_{NPs}$@OA. Bragg reflections in the 2θ range 10-70° correspond to those of γ-$Fe_2O_3$ phase with cubic inverse spinel structure (PDF card 895892).

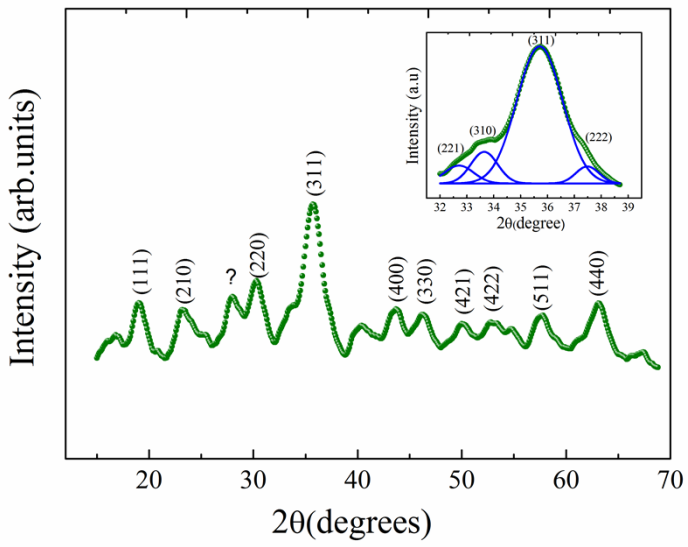


**ESI 5**: The figure shows the FTIR of the three systems in the low wavenumber region. The major peaks at 565 $cm^{-1}$ is attributed to the Fe-O stretching mode of magnetite,[4] while shoulder peaks at 450 $cm^{-1}$ and 630 $cm^{-1}$ are the signature of maghemite phase. [4]

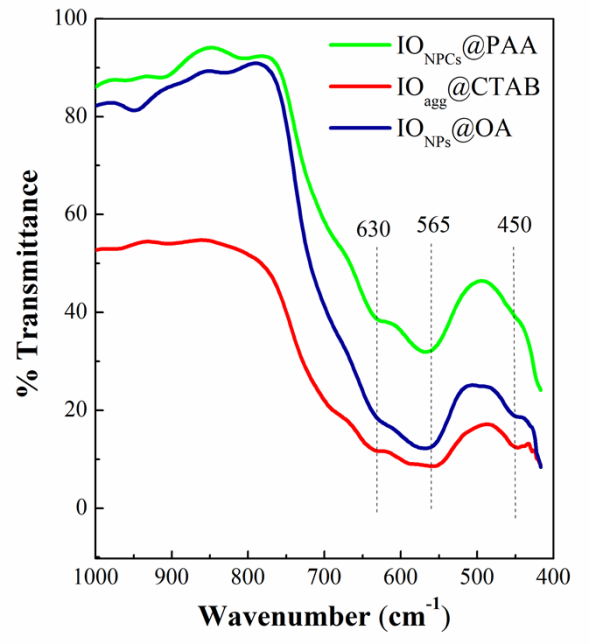

**ESI 6:** Table shows the Raman peak positions for three systems with their assignments.

| $IO_{NPs}$@OA | $IO_{agg}$@CTAB | $IO_{NPCs}$@PAA | Assignment |
|---|---|---|---|
| 194 ($T_{2g}$) | 194 ($T_{2g}$) | | magnetite |
| 302 ($E_g$) | 294[a] ($E_g$) | 303 ($E_g$) | magnetite |
| 375($E_g$) | 356 ($E_g$) | 366 ($E_g$) | maghemite |
| | 425 [b] (Eg) | | magnetite |
| 484 ($T_{2g}$) | 494[c] ($T_{2g}$) | 480($T_{2g}$) | magnetite |
| 664 ($A_{1g}$) | 663 ($A_{1g}$) | 664($A_{1g}$) | magnetite |
| 714($A_{1g}$) | 723 ($A_{1g}$) | 714($A_{1g}$) | maghemite |

**References:**


[1] L. Zhang, R. He, and H.C. Gu, *Appl. Surf. Sci.,* 2006, **253**, 2611.

[2] H.M. Yang, H. J. Lee, K.S. Jang, C. W. Park, H. W. Yang, W. D. Heo and J.D. Kim, *J. Mater. Chem.*, 2009, **19**, 4566.

[3] A. Hofmann, S. Thierbach, A. Semisch, A. Hartwig, M. Taupitz, E. Ruhl and C. Graf, *J. Mater. Chem*., 2010, **20**, 7842.

[4] S. Nasrazadani and H. Namduri, *Spectrochimica Acta Part B*, 2006, **61**, 565.